




Evolution of the electronic structure and correlations accompanied by suppression of itinerant ferromagnetism in $\text{Sr}_{1-x}(\text{La}_{0.5}\text{K}_{0.5})_x\text{RuO}_3$

Ikuto Kawasaki ^{1,*}, Shin-ichi Fujimori,¹ Yukiharu Takeda,¹ Hiroshi Yamagami ^{1,2}, Rahmanto,^{3,4} Yutoku Honma,^{3,4} Kensuke Matsuoka,^{3,4} and Makoto Yokoyama ^{3,4}

¹Materials Sciences Research Center, Japan Atomic Energy Agency, Sayo, Hyogo 679-5148, Japan

²Department of Physics, Faculty of Science, Kyoto Sangyo University, Kyoto 603-8555, Japan

³Faculty of Science, Ibaraki University, Mito, Ibaraki 310-8512, Japan

⁴Institute of Quantum Beam Science, Ibaraki University, Mito, Ibaraki 310-8512, Japan



(Received 24 June 2021; revised 1 March 2022; accepted 20 April 2022; published 16 May 2022)

We have carried out soft x-ray photoemission experiments on itinerant ferromagnet $\text{Sr}_{1-x}(\text{La}_{0.5}\text{K}_{0.5})_x\text{RuO}_3$ to investigate how the electronic state varies with doping concentration. The Ru $4d$ -derived coherent part of the valence spectra develops significantly with increasing x for $x \leq 0.3$, which can be explained by the suppression of the ferromagnetic exchange splitting. With further increasing x , this development is overwhelmed by the spectral weight transfer from the coherent to the incoherent parts due to the electron correlation. The enhancement of the electron correlation effect with doping is also confirmed by the Ru $3d$ core-level spectra as the suppression of the well-screened peak. In contrast to the remarkable variation of the Ru $4d$ spectral intensity as a function of x , the valence spectra hardly depend on temperature and do not show any noticeable change across the magnetic transition temperatures, indicating that the temperature dependence of the exchange splitting cannot be explained by a simple Stoner picture. We compare the present photoemission results with those for isostructural $\text{Sr}_{1-x}\text{A}_x\text{RuO}_3$ ($A = \text{La}$ and Ca) and discuss the origin of the difference in the magnetic property between these doped compounds.

DOI: [10.1103/PhysRevB.105.195122](https://doi.org/10.1103/PhysRevB.105.195122)

I. INTRODUCTION

Ruthenium-based oxides exhibit a variety of interesting properties, such as quantum criticality [1,2], non-Fermi-liquid behavior [3], and current-induced insulator-metal transition [4]. The electron correlation among Ru $4d$ electrons in these oxides has been considered to be weak compared to their strongly correlated $3d$ counterparts. Nevertheless, the above intriguing properties demonstrate that electron correlation of the Ru $4d$ electrons plays crucial roles.

SrRuO_3 crystallizes into a GaFeO_3 -type orthorhombically distorted perovskite structure and shows a ferromagnetic (FM) order below $T_C = 160$ K with a saturation moment close to $1 \mu_B$ per formula unit [5,6]. The ordered FM moment is considered to be mainly ascribed to the itinerant Ru $4d$ electrons because the Ru $4d$ -derived components in the photoemission (PES) spectra are approximately reproduced by calculations based on a standard density functional theory (DFT) [7]. However, localized characteristics of the Ru $4d$ electrons have also been pointed out by following experimental results. The electrical resistivity exceeds the Ioffe-Regel limit for conventional metals at high temperatures, indicative of a very small mean-free path comparable to the lattice constants [8–10]. Optical spectroscopy has revealed that the charge dynamics deviates from the Fermi-liquid description [11,12]. The Rhodes-Wohlfarth parameter, the ratio of a

paramagnetic moment and a FM ordered moment, is relatively close to the localized-moment limit [13]. Moreover, the PES spectra exhibit a weak but noticeable incoherent component originating from the electron correlation [14,15], which has been reproduced by the combined calculation of DFT and dynamical mean-field theory (DMFT) [16]. Based on these results, the Ru $4d$ electrons in SrRuO_3 seem to have a dual nature; i.e., they have both itinerant and localized characteristics.

The electron correlation in SrRuO_3 can be further enhanced by chemical substitution. In fact, metal-insulator transitions have been observed in several Ru site-substituted compounds $\text{SrRu}_{1-x}\text{M}_x\text{O}_3$ ($M = \text{Mn}$, Ti , Cr , etc.) [17–22]. Substituting Ca or La for Sr cannot induce an insulating phase but similarly enhances the electron correlation [14,23], yielding fascinating magnetic and electronic properties. In $\text{Sr}_{1-x}\text{Ca}_x\text{RuO}_3$, the FM order is monotonically suppressed upon doping Ca and disappears above a critical concentration of about $x \sim 0.8$ [24]. Nuclear magnetic resonance and thermodynamic investigations have revealed the presence of non-Fermi-liquid behavior induced by FM quantum critical fluctuations around the critical concentration [25–27]. Muon-spin-relaxation (μSR) experiments demonstrated that a phase separation between FM and nonmagnetic regions occurs at around the critical concentration [28,29]. In this μSR study, it was discussed that this phase separation is associated with the characteristics of a first-order quantum phase transition, by which the quantum critical fluctuations seem to be suppressed to some extent. Substituting La for Sr similarly suppresses

*kawasaki.ikuto@jaea.go.jp

the FM order but leads to different magnetic and electronic states [30,31]. Ac susceptibility and μ SR experiments for $\text{Sr}_{1-x}\text{La}_x\text{RuO}_3$ have shown that T_C decreases more rapidly with x , and the FM ordered state changes into a cluster-glass state [32,33]. The development of electron correlation with La concentration was confirmed by PES experiments [23]. In contrast to Ca-doped SrRuO_3 , there does not exist any prominent feature related to the FM quantum critical fluctuations in the low-temperature specific heat [32]. Therefore, the FM quantum critical point of La-doped SrRuO_3 is considered to be smeared and blurred by the development of the cluster-glass state.

The abovementioned difference between Ca- and La-doped SrRuO_3 seems to be related to the carrier doping effect by doping La: no carrier doping is expected for Ca-doped SrRuO_3 in terms of the number of valence electrons, but doping La induces an electron doping. In order to confirm this conjecture, recently we have synthesized another mixed compound $\text{Sr}_{1-x}(\text{La}_{0.5}\text{K}_{0.5})_x\text{RuO}_3$ [34] and carried out magnetic and thermal experiments [35]. The total number of valence electrons of $\text{La}_{0.5}\text{K}_{0.5}$ is equivalent to that for Ca, and therefore, no carrier doping is expected for $\text{La}_{0.5}\text{K}_{0.5}$ -doped SrRuO_3 . It was found that the FM order is suppressed as a function of x and disappears at around the critical concentration $x = 0.5$. The FM ordered state changes to a cluster-glass state, before reaching the critical concentration, and no prominent feature ascribed to the FM quantum critical fluctuations was observed in specific heat as in La-doped SrRuO_3 . Therefore, there still exists a qualitative difference concerning the electronic and magnetic properties around the critical concentration between Ca- and $\text{La}_{0.5}\text{K}_{0.5}$ -doped SrRuO_3 , which is considered to be due to the difference in the Ru $4d$ electronic state. In this study, we have performed PES experiments using bulk-sensitive soft x rays [36,37] on $\text{La}_{0.5}\text{K}_{0.5}$ -doped SrRuO_3 in order to understand the origin of the abovementioned difference between $\text{Sr}_{1-x}\text{A}_x\text{RuO}_3$ ($A = \text{Ca}, \text{La}, \text{and } \text{La}_{0.5}\text{K}_{0.5}$) from the perspective of the Ru $4d$ electronic state.

II. EXPERIMENTAL DETAILS

Polycrystalline samples of $\text{Sr}_{1-x}(\text{La}_{0.5}\text{K}_{0.5})_x\text{RuO}_3$ were synthesized by a conventional solid-state reaction method. The details of sample preparation are described in Ref. [35]. The PES and x-ray absorption spectroscopy (XAS) were carried out at the soft x-ray undulator beamline BL23SU [38] in SPring-8. Various photon energies in the soft x-ray range ($h\nu = 500$ to 1100 eV) were used. The energy distribution of photoelectrons was measured using a Gammadata-Scienta SES2002 analyzer. The total energy resolutions were approximately 60 meV for 500-eV photons and 175 meV for 1100-eV photons. The binding energy of the PES spectra was calibrated with respect to the Fermi edge (E_F) of an evaporated gold film. Clean sample surfaces were prepared by fracturing *in situ* just before the measurements. The sample temperature was controlled by a liquid helium flow cryostat and maintained at 25 K except for the temperature-dependence measurements. The base pressure of the main chamber was kept better than 1.2×10^{-8} Pa at 25 K and was temporarily increased up to around 5×10^{-8} Pa in the temperature-dependence measurements.

III. RESULTS

Figure 1(a) shows the PES spectra of the Ru $3d$ core-level for $\text{Sr}_{1-x}(\text{La}_{0.5}\text{K}_{0.5})_x\text{RuO}_3$. The Ru $3d_{5/2}$ peak clearly consists of two components as indicated by the arrows. They are referred to as well-screened and poorly screened peaks and transitions to different final states, and the positions of these peaks are identified by the minima in the second derivatives of the spectra (not shown). According to the calculation based on the DMFT, the well-screened peak originates from the screening of a core hole by itinerant quasiparticles on the Fermi surface, and its intensity decreases with decreasing the quasiparticle weight Z , defined by $Z^{-1} = 1 - \partial \text{Re} \Sigma(\omega) / \partial \omega$, where $\Sigma(\omega)$ is the self-energy due to the electron correlation effect [39]. As seen in Fig. 1(a), there is a spectral weight transfer from the well-screened peak to the poorly screened peak induced by doping La and K, reflecting an enhancement of the electron correlation in the doped samples. A similar spectral weight transfer has been reported for Ca-doped SrRuO_3 [14]. One may consider that the suppression of the well-screened peak is a consequence of the disorder effect induced by doping La and K. In order to confirm how the spectra are affected by the disorder effect, we display the spectra of the Sr $3p_{3/2}$ core-level in Fig. 1(b), which is located in the vicinity of the Ru $3d$ core-level; the peak width does not increase upon doping. The inset of Fig. 1(b) plots the residual resistivity ratio $\text{RRR} = \rho(300 \text{ K}) / \rho(4.2 \text{ K})$, where $\rho(300 \text{ K})$ and $\rho(4.2 \text{ K})$ are the values of resistivity measured at 300 and 4.2 K, respectively [35]. As seen in this inset, the RRR value, which is one metric of the disorder, does not exhibit a systematic change as a function of x for $x \geq 0.1$. These results show that the suppression of the well-screened peak with doping is not caused by the disorder effect. For a quantitative evaluation, we show the relative fraction of the poorly screened peak intensity $I_{\text{poor}} / (I_{\text{well}} + I_{\text{poor}})$ in Fig. 1(c), where I_{poor} and I_{well} are the spectral intensities at the peak positions of poorly screened and well-screened components. As shown in Fig. 1(c), the spectral weight transfer proceeds monotonically as a function of x .

In Fig. 2(a), we show the valence spectra of $\text{Sr}_{1-x}(\text{La}_{0.5}\text{K}_{0.5})_x\text{RuO}_3$ measured at 25 K and $h\nu = 700$ eV. At this temperature, the samples for $x \leq 0.3$ and for $x = 0.4$ are in the ferromagnetic and weakly disordered ferromagnetic states [35]. In contrast, the valence spectrum for $x = 0.5$ was measured in a paramagnetic phase since the ferromagnetic order of $\text{Sr}_{1-x}(\text{La}_{0.5}\text{K}_{0.5})_x\text{RuO}_3$ is fully suppressed for this doping concentration. These differences, however, do not complicate the interpretation of the valence spectra because the PES spectra exhibit almost no temperature dependence as shown later in this article. In this soft x-ray range, the Ru $4d$, O $2p$, and La $5d$ orbitals have relatively large PES cross sections, but the intensities for other orbitals, such as Ru $5s$, Sr $5s$, and La $6s$, are negligibly weak [40]. The valence spectrum for $x = 0$ is essentially the same as the spectra in previous PES studies in the soft x-ray range [14,15,23]. The PES spectra shown in Fig. 2(a) are mainly dominated by the Ru $4d$ and O $2p$ orbital components. For comparison, we carried out band structure calculations for SrRuO_3 as well as LaRuO_3 , assuming paramagnetic states. These calculations are based on a full potential version of a

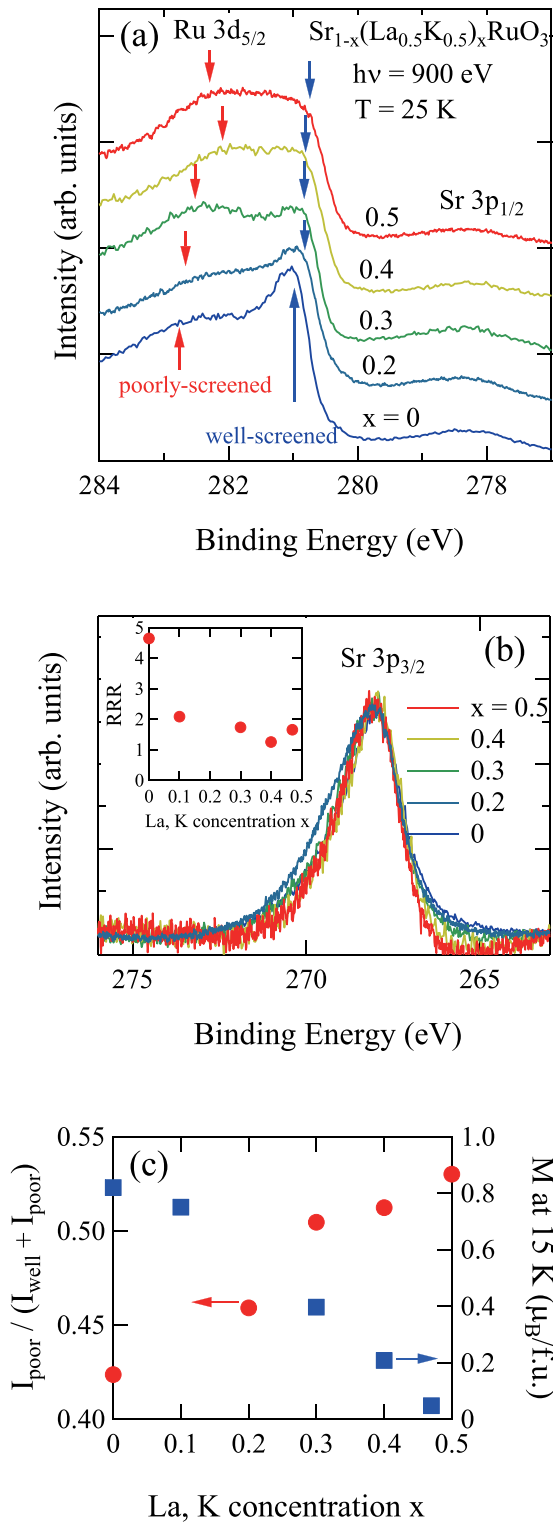


FIG. 1. (a) Ru 3d core-level photoemission spectra of $\text{Sr}_{1-x}(\text{La}_{0.5}\text{K}_{0.5})_x\text{RuO}_3$. (b) Sr 3p_{3/2} core-level spectra. The inset shows the residual resistivity ratio $\text{RRR} = \rho(300 \text{ K})/\rho(4.2 \text{ K})$ as a function of x [35]. (c) The relative fraction of the poorly screened peak intensity $I_{\text{poor}}/(I_{\text{well}} + I_{\text{poor}})$ as a function of x together with the dc magnetization measured at 15 K under a magnetic field of $B = 0.5 \text{ T}$ [35].

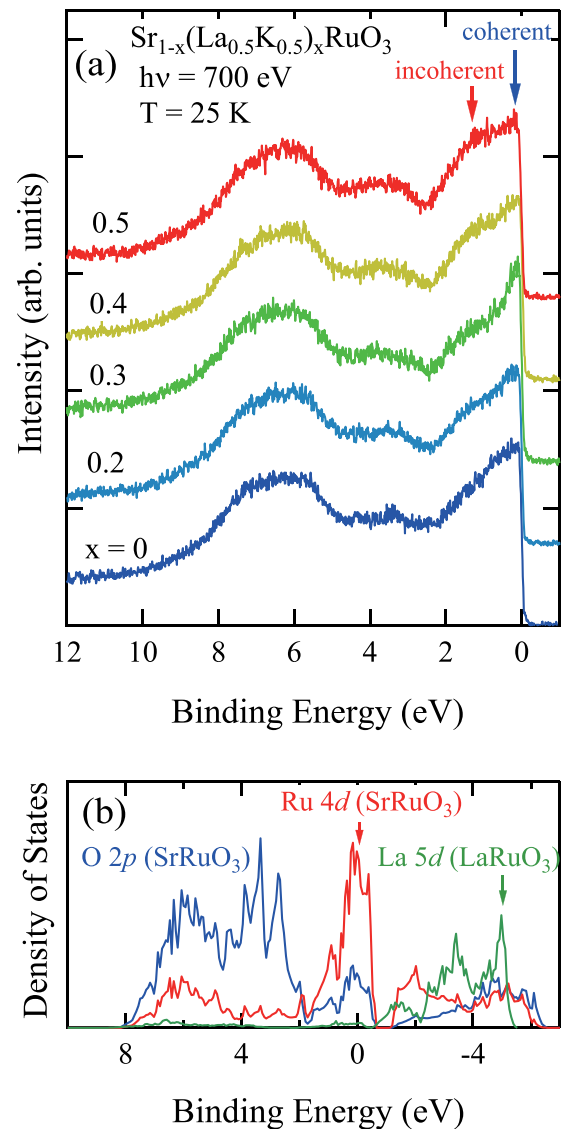


FIG. 2. (a) Valence band spectra of $\text{Sr}_{1-x}(\text{La}_{0.5}\text{K}_{0.5})_x\text{RuO}_3$ measured at 25 K and $h\nu = 700$ eV. The positions of coherent and incoherent parts are indicated by arrows. (b) Calculated partial density of states for SrRuO₃ and LaRuO₃.

Dirac-type linearized augmented plane-wave method within a local density approximation [41], and the experimental lattice constants for SrRuO₃ were used in both calculations [42]. Figure 2(b) shows the calculated partial density of states for the Ru 4d and O 2p components for SrRuO₃ and the La 5d component for LaRuO₃. The calculation for LaRuO₃ can be used as a reference point for the argument of the La 5d electronic state in $\text{Sr}_{1-x}(\text{La}_{0.5}\text{K}_{0.5})_x\text{RuO}_3$; this calculation thus employs the lattice constants of SrRuO₃ because the lattice constants for $\text{Sr}_{1-x}(\text{La}_{0.5}\text{K}_{0.5})_x\text{RuO}_3$ are relatively close to those for SrRuO₃ for small x values. The calculated La 5d and La 6s (not shown) states are almost empty, reflecting a nearly trivalent character of La atoms. According to the calculation for SrRuO₃, the experimental spectral

intensity extending from E_F to around 2 eV mainly originates from the Ru 4*d* orbital, and the spectral intensity from 2 to 10 eV is attributed to the O 2*p* orbital. The contribution of the La 5*d* orbital for the PES spectrum is thought to be much smaller than the contributions of the Ru 4*d* and O 2*p* orbitals. This is because the number of La 5*d* electrons is expected to be small and, in fact, is estimated to be 0.33 for formula units of LaRuO₃ in the above calculation.

It has been suggested by previous PES studies for SrRuO₃ that the spectral weight just below E_F is the coherent part, and the broad spectral intensity at around 1.2 eV is attributed to the incoherent part [7,14,15,23]. This incoherent part has been reproduced by the DMFT calculation [16]; the Coulomb interaction parameter U in the Hamiltonian of this DMFT calculation was set to be $U = 3$ eV. On the other hand, according to the detailed PES study by Grebinskij *et al.*, the spectral weight at 1.2 eV for SrRuO₃ may partially be due to the finite admixture of O 2*p* and the asymmetric shape of the coherent Ru 4*d* component [7]. This indicates that the electron correlation effect in SrRuO₃ is not so strong. One can see that the spectral shape of Ru 4*d* shows a nonmonotonic change as a function of x . We consider that this evolution of the spectral shape by doping La and K is not caused by the change of the on-site Coulomb interaction but by the changes in the magnitude of the hybridization effect and/or the band structure since the strength of the on-site Coulomb interaction should be determined mostly by the atomic potential of an Ru atom. The coherent part of SrRuO₃ becomes sharper with increasing x for $x \leq 0.3$. This behavior is considered to be ascribed to the suppression of the exchange splitting between the majority and minority spin bands because such a development of the density of states near E_F has been reproduced by DFT calculations [14]. In Fig. 1(c), we also display the low-temperature dc magnetization under a magnetic field of $B = 0.5$ T, which can be regarded as a good measure of the strength of the exchange splitting [35]. According to the data shown in Fig. 1(c), the exchange splitting decreases monotonically with doping. Meanwhile, the intensity of the coherent part starts to decrease with increasing x for $x \geq 0.3$ and is transferred to the incoherent part. In this concentration region, the abovementioned effect of the suppression of the exchange splitting seems to be overwhelmed by the renormalization factor $Z = (1 - \partial \text{Re} \Sigma(\omega) / \partial \omega)^{-1}$ caused by the electron correlation, which suppresses the coherent part. The data shown Fig. 1(c) indicate that both the exchange splitting and the electron correlation effect change monotonically with doping. Therefore, the nonmonotonic change of the valence band spectra should be due to complex interplay between the renormalization factor and the suppression of the exchange splitting. Here, we would like to stress that the development of the incoherent part is unlikely to be caused by the disorder effect induced by doping La and K, because, as we mentioned before, RRR does not show a systematic dependence on x for $x \geq 0.1$ [inset of Fig. 1(b)]. Note that the observed variation of the Ru 4*d* spectral shape is consistent not only with the Ru 3*d* core-level spectra but also with the specific heat results [35], in which the electronic specific heat coefficient increases with x , since both the suppression of the exchange splitting and the development of electron correlation enhance the density of states at E_F . Moreover, the energy position of the incoherent component observed for $x \geq 0.4$ is nearly

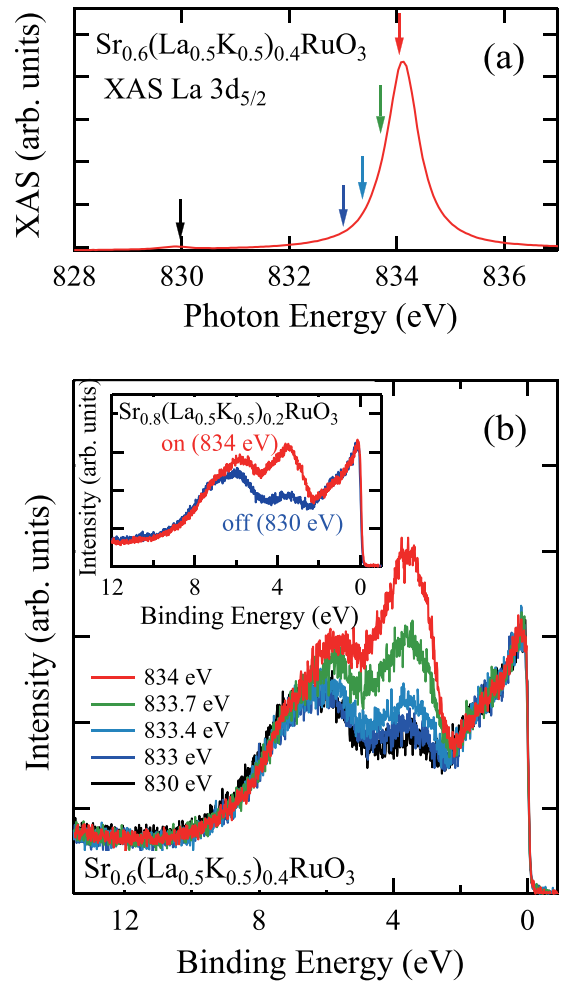


FIG. 3. (a) The x-ray absorption spectrum and the positions of the employed photon energies in the resonance PES for $\text{Sr}_{1-x}(\text{La}_{0.5}\text{K}_{0.5})_x\text{RuO}_3$, with $x = 0.4$. (b) Valence band spectra near the La 3*d*_{5/2} core absorption edge for $x = 0.4$. These spectra were normalized by the spectral intensity around E_F . The inset displays the on- and off-resonance spectra for $x = 0.2$ where the on-resonance spectrum is measured at the peak energy of the La 3*d*_{5/2} XAS spectrum (not shown).

the same as the energy positions for other correlated Ru oxides, such as CaRuO₃, Sr_{1-x}Ca_xRuO₃, and Sr_{1-x}La_xRuO₃ [14,23,43].

One may consider that the observed spectral change of Ru 4*d* components is partially due to the La 5*d* spectral intensity. In order to check this, we have carried out La 3*d*-edge-resonance PES experiments, by which the La 5*d* spectral weight can be selectively enhanced [44]. There are two processes in the La 3*d*-edge-resonance PES:

$$3d^{10}4f^05d^n + h\nu \rightarrow 3d^{10}4f^05d^{n-1} + e^-, \quad (1)$$

$$3d^{10}4f^05d^n + h\nu \rightarrow 3d^94f^15d^n \rightarrow 3d^{10}4f^05d^{n-1} + e^-, \quad (2)$$

where e^- represents a photoelectron. These processes are known as the (1) direct and (2) Auger processes. They have the same initial and final states, and therefore, the La 5*d* contribution can be resonantly enhanced. Figure 3(a) shows

the La $3d_{5/2}$ XAS spectrum for $\text{Sr}_{1-x}(\text{La}_{0.5}\text{K}_{0.5})_x\text{RuO}_3$, with $x = 0.4$, and the positions of the employed photon energies in the resonant PES, which are indicated by arrows. In Fig. 3(b), we display the valence spectra near the La $3d_{5/2}$ core absorption edge for $x = 0.4$. We found that the spectral weight from 2 to 7 eV for $x = 0.4$ is enhanced with approaching the peak energy in the XAS spectrum, suggesting that the La $5d$ states mainly hybridize with the O $2p$ states. In contrast, the spectral weight from E_F to 2 eV does not exhibit any enhancement. The inset of Fig. 3(b) shows the on- and off-resonance spectra for $x = 0.2$. This result confirms that the energy distribution of the La $5d$ state of $\text{Sr}_{1-x}(\text{La}_{0.5}\text{K}_{0.5})_x\text{RuO}_3$ hardly depends on the value of x . Hence, the observed spectral shape evolution for Ru $4d$ in Fig. 2(a) as a function of x is not influenced by the La $5d$ states. Note that the presence of the La $5d$ contribution indicates that the electronic state of $\text{Sr}_{1-x}(\text{La}_{0.5}\text{K}_{0.5})_x\text{RuO}_3$ deviates from a simple ionic picture and the calculated result for LaRuO_3 in Fig. 2(b) to some extent, in which the La atoms are nearly trivalent and the La $5d$ states are almost empty. One possible explanation for this discrepancy is that in $\text{Sr}_{1-x}(\text{La}_{0.5}\text{K}_{0.5})_x\text{RuO}_3$ the hybridization between O $2p$ and La $5d$ is much more enhanced compared to the calculation for LaRuO_3 by the local crystallographic disorder around La atoms, and as a result the O $2p$ bands partially acquire a La $5d$ -orbital character. The similar deviation from the simple ionic picture was also reported in our previous PES and magnetization experiments for La-doped SrRuO_3 [23,35].

The PES spectra in the present study are expected to mainly reflect the bulk electronic states because of the use of bulk-sensitive soft x-ray photons. However, our previous PES experiments for La-doped SrRuO_3 have shown that the electronic state in the surface region is markedly different from that of the bulk region [23]. Here, in order to investigate the bulk electronic state, we subtract the surface state by following the procedure given in Ref. [14]. The PES spectra are assumed to consist of bulk and surface components as follows:

$$I(E) = I_{\text{surface}}(E)(1 - e^{-d/\lambda}) + I_{\text{bulk}}(E)e^{-d/\lambda}, \quad (3)$$

where I_{surface} and I_{bulk} represent the spectral intensities of the bulk and surface regions, respectively. d and λ are the thickness of the surface layer and the photoelectron mean-free path. We have used the λ values of 10 and 19 Å for $h\nu = 500$ and 1100 eV, which are obtained from the semiempirical expressions for the mean-free path [45]. One can extract the I_{surface} and I_{bulk} from the PES spectra measured at two different photon energies. Figures 4(a) and 4(b) show the PES spectra of $\text{Sr}_{1-x}(\text{La}_{0.5}\text{K}_{0.5})_x\text{RuO}_3$ measured at $h\nu = 500$ and 1100 eV, where the O $2p$ contributions are subtracted by fitting them by multiple Gaussians, and therefore, these spectra consist only of Ru $4d$ orbitals. The spectra measured at $h\nu = 500$ eV are convoluted with a Gaussian to eliminate the energy resolution difference between $h\nu = 500$ and 1100 eV. The surface thickness is tentatively assumed to be 6 Å, which is comparable to the dimension of the unit cell [35]. Figures 4(c) and 4(d) show the obtained bulk and surface spectra for $\text{La}_{0.5}\text{K}_{0.5}$ -doped SrRuO_3 . One can recognize that the incoherent part (~ 1.2 eV) is markedly enhanced in the surface region. The simplest explanation is that the surface atoms have fewer near-

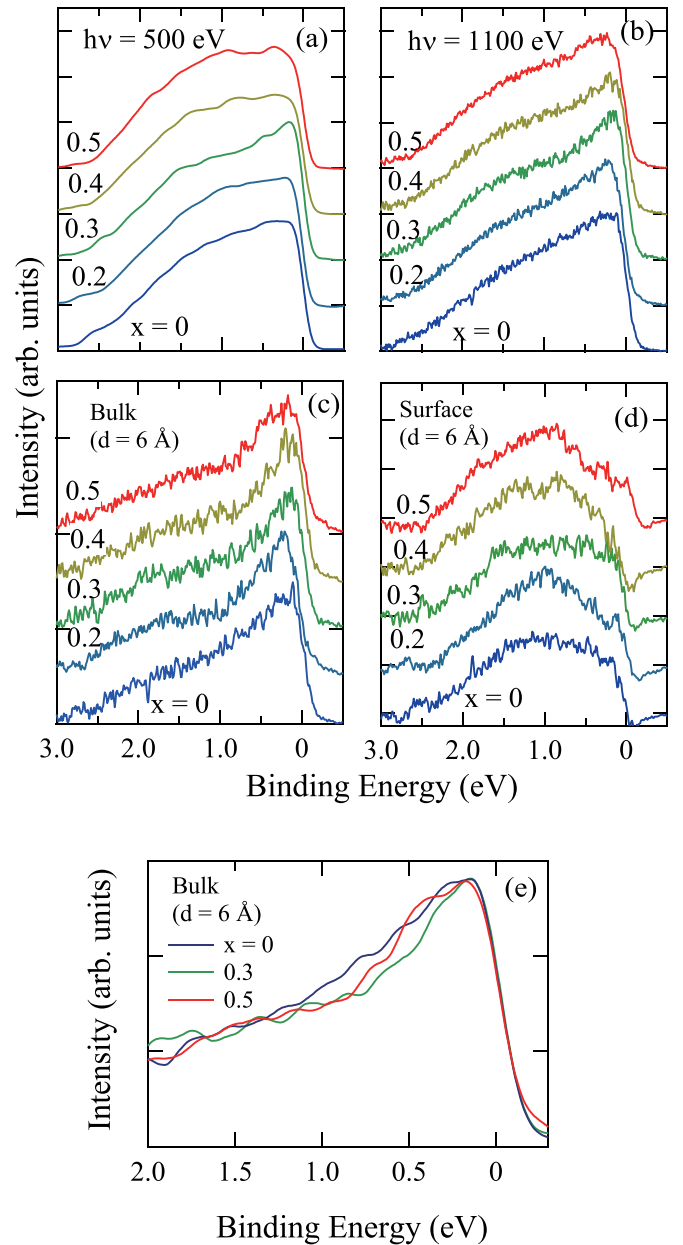


FIG. 4. (a) and (b) The Ru $4d$ spectral weights extracted from PES spectra at $h\nu = 500$ and 1100 eV, where the O $2p$ components are subtracted. These spectra are normalized by the area of each spectrum. (c) and (d) The bulk and surface contributions obtained by using Eq. (3). (e) Comparison of the bulk contributions for $x = 0, 0.3$, and 0.5 , where these spectra are normalized by intensity around E_F and are smoothed by a Gaussian function whose width is narrower than the energy resolution.

hybridized. The sharpening and enhancement of the coherent part for $x = 0.3$ seen in Fig. 2(a) become less noticeable in Fig. 4(c). However, as seen in Fig. 4(e), where we overlay the bulk spectra, the bulk spectra also show the sharpening of the coherent part at $x = 0.3$, suggesting that the aforementioned arguments about the results for Fig. 2(a) are applicable for the bulk electronic state of $\text{Sr}_{1-x}(\text{La}_{0.5}\text{K}_{0.5})_x\text{RuO}_3$. To confirm the robustness of the above analysis against the estimation error in d , we have performed the same analyses using different

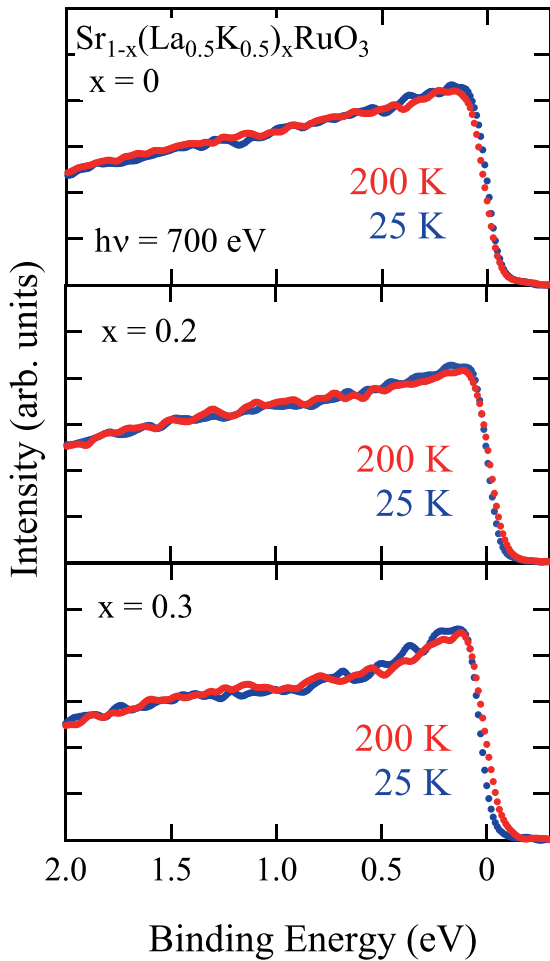


FIG. 5. Temperature dependence of the valence band spectra for $\text{Sr}_{1-x}(\text{La}_{0.5}\text{K}_{0.5})_x\text{RuO}_3$ measured at $h\nu = 700$ eV. These spectra are broadened by a Gaussian function whose width is smaller than the energy resolution to improve the statistics.

values of d and shown that the shapes of bulk spectra do not exhibit any noticeable change for the d value range of 6–12 Å (not shown).

Next, we have investigated the temperature dependence of the valence spectra to study how the electronic state changes across the magnetic transition temperature. Figure 5 displays the PES spectra for $x \leq 0.3$ measured at 25 and 200 K. The ferromagnetic ordering temperatures for $x = 0, 0.2,$ and 0.3 were reported as 161, 120, and 82 K, respectively [35]. As shown in Fig. 5, we did not observe any noticeable temperature dependence of the spectra. We also measured the temperature dependence of the PES spectra for $x = 0.4$ and 0.5 and confirmed that their PES spectra also hardly depend on temperature (not shown).

IV. DISCUSSION

In this study, we have revealed that the Ru 4*d* electronic state for $\text{Sr}_{1-x}(\text{La}_{0.5}\text{K}_{0.5})_x\text{RuO}_3$ markedly evolves as a function of x . The observed development of the coherent part in the valence spectra with x for $x \leq 0.3$ can naturally be explained by the suppression of the exchange splitting as

described in the previous section. On the other hand, the valence spectra for $x \geq 0.3$ and Ru 3*d* core-level spectra clearly indicate a development of the electron correlation effect. Similar developments of the electron correlation have also been confirmed in Ca- and La-doped SrRuO_3 by PES experiments [14,23]. However, as described in the Introduction, these doped systems $\text{Sr}_{1-x}\text{A}_x\text{RuO}_3$ ($A = \text{Ca}, \text{La},$ and $\text{La}_{0.5}\text{K}_{0.5}$) exhibit different magnetic properties. In this section, we discuss the possible origin of this difference in terms of the Ru 4*d* electronic state.

First, we compare the magnetic and electronic properties between La- and $\text{La}_{0.5}\text{K}_{0.5}$ -doped SrRuO_3 . Their FM ordering temperatures are suppressed by doping in both cases, and the FM ordered states are replaced by cluster-glass states before reaching the critical concentration, at which the magnetic ordering temperature drops to zero [32,35]. According to the ac magnetic susceptibility measurements, the magnetic ordering process of the cluster-glass states as a function of temperature is no longer a well-defined second-order phase transition but rather a gradual spin freezing. This provides an explanation for the absence of the prominent enhancement in the low-temperature specific heat due to quantum critical fluctuations in these systems. It is natural to consider that the emergence of the cluster-glass states is related to disorder induced by doped ions and that the FM droplets are stabilized at nanosized Sr-rich regions. Note that unit-cell volumes for La- and $\text{La}_{0.5}\text{K}_{0.5}$ -doped SrRuO_3 are almost identical for a given dopant concentration [35], indicating that both the compounds have very similar local heterogeneity of Sr atom distribution.

Despite the above similarity between La- and $\text{La}_{0.5}\text{K}_{0.5}$ -doped SrRuO_3 , there is a quantitative difference in their magnetic and electronic properties as follows. The FM ordered state of La-doped SrRuO_3 changes to the cluster-glass state already at $x = 0.3$, whereas for $\text{La}_{0.5}\text{K}_{0.5}$ -doped SrRuO_3 , a higher x value ($x \geq 0.45$) is required to induce the cluster-glass ordering [32,35]. Therefore, the magnetic ordered state for La-doped SrRuO_3 seems to be more sensitive to the local heterogeneity compared to $\text{La}_{0.5}\text{K}_{0.5}$ -doped SrRuO_3 . Figure 6 shows the comparison between the valence spectrum of $\text{Sr}_{0.5}(\text{La}_{0.5}\text{K}_{0.5})_{0.5}\text{RuO}_3$ and that for $\text{Sr}_{0.5}\text{La}_{0.5}\text{RuO}_3$ cited from our previous work [23]. As seen in this figure, the incoherent part for La-doped SrRuO_3 is more developed than that for $\text{La}_{0.5}\text{K}_{0.5}$ -doped SrRuO_3 , suggesting a stronger electron correlation and localized character of the Ru 4*d* electrons in the former compound. One possible explanation for the abovementioned difference in the magnetic properties is that the evolution toward the cluster-glass state is partially stimulated by the electron correlation effect among Ru 4*d* electrons.

In $\text{Sr}_{1-x}\text{Ca}_x\text{RuO}_3$, an evolution of FM quantum critical fluctuations at around the critical concentration has been observed by various experimental probes [25–27]. Moreover, μSR studies confirmed the occurrence of a phase separation between FM ordered and paramagnetic volumes around the critical concentration, which seems to be associated with the first-order quantum phase transition [28,29]. These results demonstrate that the FM transitions for Ca-doped SrRuO_3 keep the characteristics of well-defined first- or second-order phase transitions up to the critical concentration range and that the FM ordered state is less affected by the local

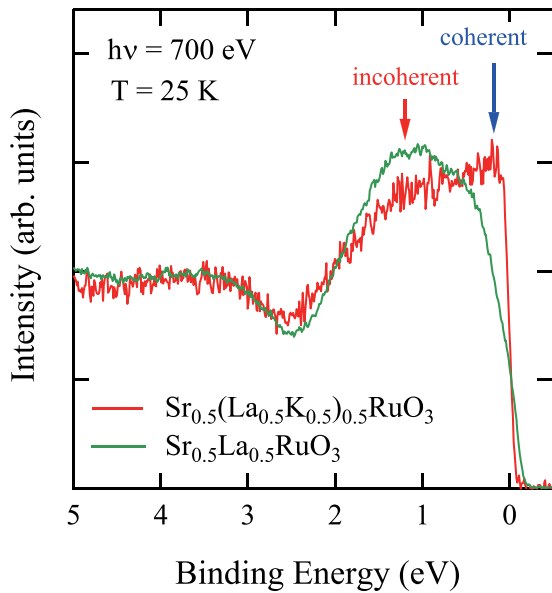


FIG. 6. Comparison of the valence band spectra between $\text{Sr}_{1-x}(\text{La}_{0.5}\text{K}_{0.5})_x\text{RuO}_3$ and $\text{Sr}_{1-x}\text{La}_x\text{RuO}_3$ with $x = 0.5$ at 25 K and $h\nu = 700$ eV. The latter spectrum is taken from Ref. [23].

heterogeneity. If the abovementioned conjecture about the relation between the emergence of the cluster-glass state and the electron correlation effect is valid, the electron correlation for Ca-doped SrRuO_3 should be weaker compared to that for La- and $\text{La}_{0.5}\text{K}_{0.5}$ -doped SrRuO_3 . The previous PES experiments in the soft x-ray range for $\text{Sr}_{1-x}\text{Ca}_x\text{RuO}_3$ have observed a weak but well-resolved peak due to the coherent part in the valence spectra for $x = 0.6$ [14], whereas a peak structure is not discernible in $\text{Sr}_{1-x}\text{A}_x\text{RuO}_3$ ($A = \text{La}$ and $\text{La}_{0.5}\text{K}_{0.5}$) for $x = 0.5$ as shown in Fig. 6 despite the smaller x value and the better energy resolutions of the latter PES experiments. This feature indicates the weaker effect of the renormalization factor $Z = (1 - \partial\text{Re}\Sigma(\omega)/\partial\omega)^{-1}$ in Ca-doped SrRuO_3 and is consistent with our above conjecture.

Finally, we discuss the physical implications of the temperature-independent valence spectra for $\text{Sr}_{1-x}(\text{La}_{0.5}\text{K}_{0.5})_x\text{RuO}_3$. X-ray magnetic circular dichroism measurements performed for SrRuO_3 have shown that the orbital moments are quenched, and the FM order is mainly caused by spin moments [46,47]. Hence, to reproduce the ordered moment size of $\sim 1 \mu_B$ [5,6], a large amount of exchange splitting between majority and minority bands is required, and in fact, its energy scale is estimated to be

around 0.5 eV by DFT calculations [48]. The observed dramatic development of the coherent part in the valence spectra with x for $x \leq 0.3$ is naturally explained by the suppression of this exchange splitting in SrRuO_3 . Therefore, the absence of the temperature dependence of the valence spectra across the FM transitions for $\text{Sr}_{1-x}(\text{La}_{0.5}\text{K}_{0.5})_x\text{RuO}_3$ is quite remarkable and is indicative of the breakdown of a simple Stoner picture, in which the exchange splitting disappears above the Curie temperature. This puzzling result is consistent with angle-resolved PES and optical spectroscopy studies for SrRuO_3 , which suggest that the exchange splitting persists above the Curie temperature and the long-range FM order is destroyed in the paramagnetic phase by the spatial and temporal fluctuations of the exchange splitting [49,50]. Presence of the residual exchange splitting in the paramagnetic phase is reproduced by the DFT+DMFT calculation [16].

V. CONCLUSION

We have studied how the electronic state of $\text{Sr}_{1-x}(\text{La}_{0.5}\text{K}_{0.5})_x\text{RuO}_3$ evolves with doping concentration via soft x-ray PES experiments. The Ru 4d-derived component in the PES spectra markedly changes with increasing x . The coherent part develops with x for $x \leq 0.3$ due to the ferromagnetic exchange splitting being suppressed. On the other hand, the intensity of the coherent part decreases with further increasing the dopant concentration, reflecting that the effect of the suppression of the exchange splitting is overwhelmed by the renormalization factor caused by electron correlations for $x \geq 0.3$. The results of the Ru 3d core-level PES further support this interpretation. In contrast to this x variation of the Ru 4d valence spectra, we did not observe any noticeable temperature dependence of the spectra across the magnetic transition temperatures, indicating that the temperature dependence of the exchange splitting does not follow the prediction of the simple Stoner picture. These PES results concerning the Ru 4d electronic state are compared with those for isostructural Ca- and La-doped SrRuO_3 , and we discuss the origin of the different magnetic properties between these doped compounds.

ACKNOWLEDGMENTS

This work was performed under Proposal No. 2020A23811 at SPring-8 BL23SU. This research was supported in part by JSPS KAKENHI Grants No. 17K05529 and No. 20K03852.

- [1] S. A. Grigera, R. S. Perry, A. J. Schofield, M. Chiao, S. R. Julian, G. G. Lonzarich, S. I. Ikeda, Y. Maeno, A. J. Millis, and A. P. Mackenzie, *Science* **294**, 329 (2001).
- [2] S. A. Grigera, P. Gegenwart, R. A. Borzi, F. Weickert, A. J. Schofield, R. S. Perry, T. Tayama, T. Sakakibara, Y. Maeno, A. G. Green, and A. P. Mackenzie, *Science* **306**, 1154 (2004).
- [3] P. Khalifah, N. D. Nelson, R. Jin, Z. Q. Mao, Y. Liu, Q. Huang, X. P. A. Gao, A. P. Ramirez, and R. J. Cava, *Nature (London)* **411**, 669 (2001).
- [4] C. Sow, S. Yonezawa, S. Kitamura, T. Oka, K. Kuroki, F. Nakamura, and Y. Maeno, *Science* **358**, 1084 (2017).
- [5] A. Callaghan, C. W. Moeller, and R. Ward, *Inorg. Chem.* **5**, 1572 (1966).
- [6] A. Kanbayasi, *J. Phys. Soc. Jpn.* **41**, 1876 (1976).
- [7] S. Grebinkij, S. Masys, S. Mickevičius, V. Lissauskas, and V. Jonauskas, *Phys. Rev. B* **87**, 035106 (2013).
- [8] L. Klein, J. S. Dodge, C. H. Ahn, G. J. Snyder, T. H. Geballe, M. R. Beasley, and A. Kapitulnik, *Phys. Rev. Lett.* **77**, 2774 (1996).

- [9] O. Gunnarsson, M. Calandra, and J. E. Han, *Rev. Mod. Phys.* **75**, 1085 (2003).
- [10] G. Cao, W. Song, Y. Sun, and X. Lin, *Solid State Commun.* **131**, 331 (2004).
- [11] P. Kotic, Y. Okada, N. C. Collins, Z. Schlesinger, J. W. Reiner, L. Klein, A. Kapitulnik, T. H. Geballe, and M. R. Beasley, *Phys. Rev. Lett.* **81**, 2498 (1998).
- [12] J. S. Dodge, C. P. Weber, J. Corson, J. Orenstein, Z. Schlesinger, J. W. Reiner, and M. R. Beasley, *Phys. Rev. Lett.* **85**, 4932 (2000).
- [13] F. Fukunaga and N. Tsuda, *J. Phys. Soc. Jpn.* **63**, 3798 (1994).
- [14] M. Takizawa, D. Toyota, H. Wadati, A. Chikamatsu, H. Kumigashira, A. Fujimori, M. Oshima, Z. Fang, M. Lippmaa, M. Kawasaki, and H. Koinuma, *Phys. Rev. B* **72**, 060404(R) (2005).
- [15] K. Horiba, H. Kawanaka, Y. Aiura, T. Saitoh, C. Satoh, Y. Kikuchi, M. Yokoyama, Y. Nishihara, R. Eguchi, Y. Senba, H. Ohashi, Y. Kitajima, and S. Shin, *Phys. Rev. B* **81**, 245127 (2010).
- [16] M. Kim and B. I. Min, *Phys. Rev. B* **91**, 205116 (2015).
- [17] G. Cao, S. Chikara, X. N. Lin, E. Elhami, V. Durairaj, and P. Schlottmann, *Phys. Rev. B* **71**, 035104 (2005).
- [18] R. K. Sahu, Z. Hu, M. L. Rao, S. S. Manoharan, T. Schmidt, B. Richter, M. Knupfer, M. Golden, J. Fink, and C. M. Schneider, *Phys. Rev. B* **66**, 144415 (2002).
- [19] M. Yokoyama, C. Satoh, A. Saitou, H. Kawanaka, H. Bando, K. Ohoyama, and Y. Nishihara, *J. Phys. Soc. Jpn.* **74**, 1706 (2005).
- [20] S. Kolesnik, B. Dabrowski, and O. Chmaissem, *Phys. Rev. B* **78**, 214425 (2008).
- [21] K. W. Kim, J. S. Lee, T. W. Noh, S. R. Lee, and K. Char, *Phys. Rev. B* **71**, 125104 (2005).
- [22] A. J. Williams, A. Gillies, J. P. Attfield, G. Heymann, H. Huppertz, M. J. Martínez-Lope, and J. A. Alonso, *Phys. Rev. B* **73**, 104409 (2006).
- [23] I. Kawasaki, Y. Sakon, S.-i. Fujimori, H. Yamagami, K. Tenya, and M. Yokoyama, *Phys. Rev. B* **94**, 174427 (2016).
- [24] G. Cao, S. McCall, M. Shepard, J. E. Crow, and R. P. Guertin, *Phys. Rev. B* **56**, 321 (1997).
- [25] K. Yoshimura, T. Imai, T. Kiyama, K. R. Thurber, A. W. Hunt, and K. Kosuge, *Phys. Rev. Lett.* **83**, 4397 (1999).
- [26] T. Kiyama, K. Yoshimura, K. Kosuge, H. Michor, and G. Hilscher, *J. Phys. Soc. Jpn.* **67**, 307 (1998).
- [27] C. L. Huang, D. Fuchs, M. Wissinger, R. Schneider, M. C. Ling, M. S. Scheurer, J. Schmalian, and H. v. Löhneysen, *Nat. Commun.* **6**, 8188 (2015).
- [28] Y. J. Uemura, T. Goko, I. M. Gat-Malureanu, J. P. Carlo, P. L. Russo, A. T. Savici, A. Aczel, G. J. MacDougall, J. A. Rodriguez, G. M. Luke, S. R. Dunsiger, A. McCollam, J. Arai, C. Pfleiderer, P. Böni, K. Yoshimura, E. Baggio-Saitovitch, M. B. Fontes, J. Larrea, Y. V. Sushko *et al.*, *Nat. Phys.* **3**, 29 (2007).
- [29] I. M. Gat-Malureanu, J. P. Carlo, T. Goko, A. Fukaya, T. Ito, P. P. Kyriakou, M. I. Larkin, G. M. Luke, P. L. Russo, A. T. Savici, C. R. Wiebe, K. Yoshimura, and Y. J. Uemura, *Phys. Rev. B* **84**, 224415 (2011).
- [30] R. Bouchard and J. Weiher, *J. Solid State Chem.* **4**, 80 (1972).
- [31] H. Nakatsugawa, E. Iguchi, and Y. Oohara, *J. Phys.: Condens. Matter* **14**, 415 (2002).
- [32] I. Kawasaki, M. Yokoyama, S. Nakano, K. Fujimura, N. Netsu, H. Kawanaka, and K. Tenya, *J. Phys. Soc. Jpn.* **83**, 064712 (2014).
- [33] I. Kawasaki, K. Fujimura, I. Watanabe, M. Avdeev, K. Tenya, and M. Yokoyama, *J. Phys. Soc. Jpn.* **85**, 054701 (2016).
- [34] S. Shuba, A. Mamchik, and I.-W. Chen, *J. Phys.: Condens. Matter* **18**, 9215 (2006).
- [35] R. Iwahara, R. Sugawara, Rahmanto, Y. Honma, K. Matsuoka, A. Matsuo, K. Kindo, K. Tenya, and M. Yokoyama, *Phys. Rev. Materials* **4**, 074404 (2020).
- [36] A. Sekiyama, T. Iwasaki, K. Matsuda, Y. Saitoh, Y. Ōnuki, and S. Suga, *Nature (London)* **403**, 396 (2000).
- [37] S. Tanuma, C. J. Powell, and D. R. Penn, *Surf. Interface Anal.* **43**, 689 (2011).
- [38] Y. Saitoh, Y. Fukuda, Y. Takeda, H. Yamagami, S. Takahashi, Y. Asano, T. Hara, K. Shirasawa, M. Takeuchi, T. Tanaka, and H. Kitamura, *J. Synchrotron Radiat.* **19**, 388 (2012).
- [39] H.-D. Kim, H.-J. Noh, K. H. Kim, and S.-J. Oh, *Phys. Rev. Lett.* **93**, 126404 (2004).
- [40] J. Yeh and I. Lindau, *At. Data Nucl. Data Tables* **32**, 1 (1985).
- [41] H. Yamagami, *J. Phys. Soc. Jpn.* **67**, 3176 (1998).
- [42] L. T. Nguyen, M. Abeykoon, J. Tao, S. Lapidus, and R. J. Cava, *Phys. Rev. Materials* **4**, 034407 (2020).
- [43] H. F. Yang, C. C. Fan, Z. T. Liu, Q. Yao, M. Y. Li, J. S. Liu, M. H. Jiang, and D. W. Shen, *Phys. Rev. B* **94**, 115151 (2016).
- [44] M. Y. Kimura, K. Fukushima, H. Takeuchi, S. Ikeda, H. Sugiyama, Y. Tomida, G. Kuwahara, H. Fujiwara, T. Kiss, A. Yasui, I. Kawasaki, H. Yamagami, Y. Saitoh, T. Muro, T. Ebihara, and A. Sekiyama, *J. Phys.: Conf. Ser.* **592**, 012003 (2015).
- [45] S. Tanuma, C. J. Powell, and D. R. Penn, *Surf. Sci.* **192**, L849 (1987).
- [46] J. Okamoto, T. Okane, Y. Saitoh, K. Terai, S.-I. Fujimori, Y. Muramatsu, K. Yoshii, K. Mamiya, T. Koide, A. Fujimori, Z. Fang, Y. Takeda, and M. Takano, *Phys. Rev. B* **76**, 184441 (2007).
- [47] S. Agrestini, Z. Hu, C.-Y. Kuo, M. W. Haverkort, K.-T. Ko, N. Hollmann, Q. Liu, E. Pellegrin, M. Valvidares, J. Herrero-Martin, P. Gargiani, P. Gegenwart, M. Schneider, S. Esser, A. Tanaka, A. C. Komarek, and L. H. Tjeng, *Phys. Rev. B* **91**, 075127 (2015).
- [48] K. Maiti, *Phys. Rev. B* **73**, 235110 (2006).
- [49] D. E. Shai, C. Adamo, D. W. Shen, C. M. Brooks, J. W. Harter, E. J. Monkman, B. Burganov, D. G. Schlom, and K. M. Shen, *Phys. Rev. Lett.* **110**, 087004 (2013).
- [50] D. W. Jeong, H. C. Choi, C. H. Kim, S. H. Chang, C. H. Sohn, H. J. Park, T. D. Kang, D.-Y. Cho, S. H. Baek, C. B. Eom, J. H. Shim, J. Yu, K. W. Kim, S. J. Moon, and T. W. Noh, *Phys. Rev. Lett.* **110**, 247202 (2013).